LETTER • OPEN ACCESS

Random patterns in fish schooling enhance alertness: A hydrodynamic perspective

To cite this article: U. Kadri *et al* 2016 *EPL* **116** 34002

A Letters Journal Exploring the Frontiers of Physics

November 2016

EPL, **116** (2016) 34002
doi: 10.1209/0295-5075/116/34002

www.epljournal.org

Random patterns in fish schooling enhance alertness: A hydrodynamic perspective

U. Kadri[1,2], F. Brümmer[3] and A. Kadri[4]

[1] *School of Mathematics, Cardiff University - Cardiff, CF24 4AG, UK*
[2] *Department of Mathematics, Massachusetts Institute of Technology - Cambridge, MA 02139, USA*
[3] *Institute of Biology, University of Stuttgart - Pfaffenwaldring 57, 70569 Stuttgart, Germany*
[4] *Faculty of Agricultural Sciences, Institute of Plant Breeding, Seed Science and Population Genetics, University of Hohenheim - Stuttgart, Germany*

received 7 May 2016; accepted in final form 24 November 2016
published online 12 December 2016

PACS 47.63.-b – Biological fluid dynamics
PACS 05.20.Jj – Statistical mechanics of classical fluids
PACS 87.10.Rt – Monte Carlo simulations

Abstract – One of the most highly debated questions in the field of animal swarming and social behaviour is the collective random patterns and chaotic behaviour formed by some animal species, in particular if there is a danger. Is such a behaviour beneficial or unfavourable for survival? Here we report on one of the most remarkable forms of animal swarming and social behaviour —fish schooling— from a hydrodynamic point of view. We found that some fish species do not have preferred orientation and they swarm in a random pattern mode, despite the excess of energy consumed. Our analyses, which include calculations of the hydrodynamic forces between slender bodies, show that such a behaviour may enhance the transfer of hydrodynamic information, and thus the survivability of the school could improve. These findings support the general hypothesis that a disordered and nontrivial collective behaviour of individuals within a nonlinear dynamical system is essential for optimising transfer of information —an optimisation that might be crucial for survival.

Introduction. – The concurrent movement of fish in a school involves significant hydrodynamic interactions. The relative longitudinal and lateral distances and velocities between the fish, as well as their relative lengths and cross-sectional areas determine the magnitude of the hydrodynamic forces and moments involved [1–3], which, in turn, could affect the school overall manoeuvrability [4]. It is not the aim of the current study to discuss how information due to a sudden movement is (physiologically) transferred among the school members in terms of sensory systems [5], environmental effects [6], or aerobic capacity [7]. Neither our intention is to dig into the complex aspects of the flowfield generated by the three-dimensional locomotion and the associated dynamics of complex wakes and vortices. Rather, we treat the fish as solid slender bodies moving in a potential flow. In this respect, the overall manoeuvrability of a given school is dependent of the instantaneous school structural pattern (mode) which dictates, to leading order, the hydrodynamic interactions.

Although it has been suggested that fish might be found to swim in a diamond-shape pattern to increase hydrodynamic efficiency [8], or other preferred orientations and angles, observations (fig. 1) and analyses (fig. 2) of aerial photographs and videos of different schools of fishes (Jacks, blue-lined snapper, yellow-spot emperor, goggle-eye, and bluestreak fusilier) reveal random-shape patterns instead. A comprehensive work on the shape and structural patterns in schools and swarms is found in [9], which also includes a long list of relevant references. The supporting theoretical analysis we present here shows that swimming in random modes increases the mean hydrody-

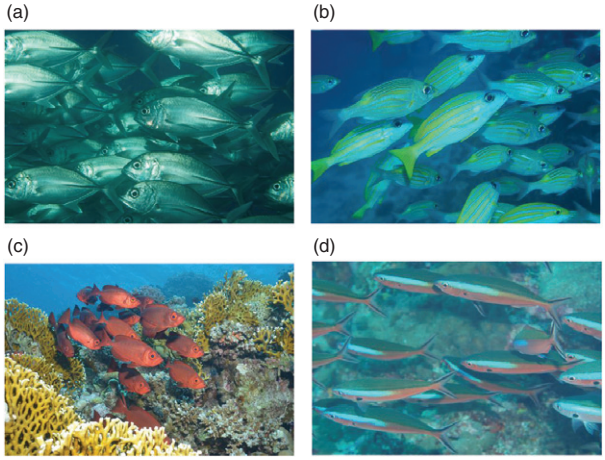

Fig. 1: (Colour online) Examples for schools of fishes swimming in random pattern mode: (a) Jack Caranx sp. (60 cm); (b) blue-lined snapper *Lutjanus kasmira* and yellow-spot emperor *Gnathodentex aurolineatus* (35 cm/24 cm); (c) goggle-eye *Priacanthus hamrur* (40 cm); and (d) bluestreak fusilier *Pterocaesio tile* (25 cm). (Photos by F. Brümmer.)

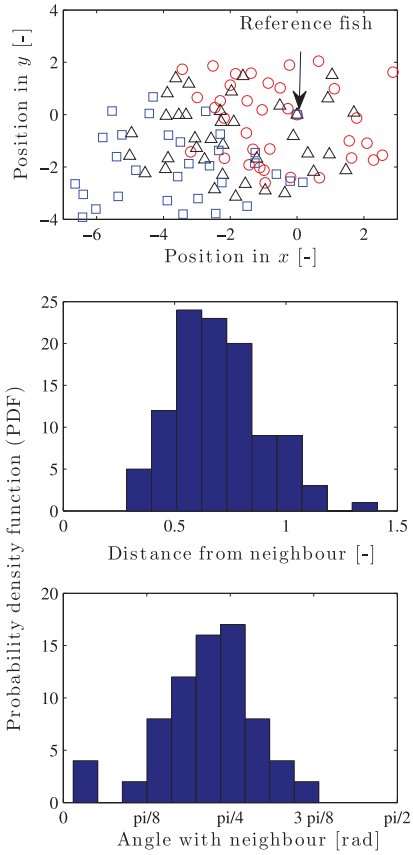

Fig. 2: (Colour online) Top: distribution of 32–36 Jack Caranx sp. (60 cm); at time 00.04.44 (circles), 00.05.44 (star), 00.06.59 (square). Middle: probability density function (PDF) of the distance between each fish and the closest upper downstream neighbour. Bottom: PDF of the angle between each fish and the closest upper downstream neighbour. All dimensionless quantities were normalized with respect to the mean fish length.

namic forces by a factor of two to five, depending on the school size. Introducing a sensitivity threshold force (*i.e.*, minimum force felt by the fish), we find that fish swimming in random modes feel the sudden change in movement of other fish at a more remote distance, which may in turn result in a decrease in the overall response time (more fish are aware of the change at any given instant) of the fish school and thus enhance the overall manoeuvring of the school. An increased energy consumption that enhances the manoeuvring efficiency is thus essential for survival especially amongst smaller fish that cannot escape fast enough from predators.

Methods. –

Hydrodynamic model. The model by [8] accurately predicts diamond-shape pattern modes especially for relatively large fish or dolphins [1,10], and for different types of fish preferred orientations might be identified. However, for smaller fish (*e.g.*, Jack Caranx sp., 60 cm) the school pattern shapes were found to be random; especially when fish encounter a danger (*e.g.*, due to the presence and sudden movement of scuba-divers) their behaviour becomes more disordered within the school; at any given instant the relative distances and angles between neighbouring fish fail to form ordered patterns, as we observed (fig. 2). It is observed that the probability density function (PDF) of the relative distances and angles are *Gaussian*, indicating continuous random variables. This observation raises the question as to whether random school patterns and disordered behaviour, which are probably due to a natural "panic" reflex [11], are beneficial or unfavourable for survival.

In order to evaluate the effect of random school patterns, we carried out a theoretical analysis, based on the studies by the authors of [12], and [13] who investigated the hydrodynamic interactions between two submerged slender bodies of revolution at various separation distances in potential flow. For the sake of brevity, the actual motion of each fish in the school is now translated into the motion of a slender ellipsoid with $d/L = \epsilon$, where d and L are the maximum lateral and longitudinal dimensions of the body, and ϵ is assumed to be small. For the potential flow past an ellipsoid moving with arbitrary velocity, the solution can be represented, equivalently, by a volume distribution of doublets, or a doublet-layer distributed over the limiting confocal ellipse, as well as by a source-layer or a doublet-layer distributed over the ellipsoid or over an interior confocal ellipsoid. Moreover, based on the singularity method, solutions for the internal flow between two confocal ellipsoids in relative motion are found (see [14]). On this basis, an approximate solution is sought for the hydrodynamic quantities of interest. Each two streamlined bodies move through an ideal fluid with constant velocities U_i and U_j along parallel paths. The relative po-

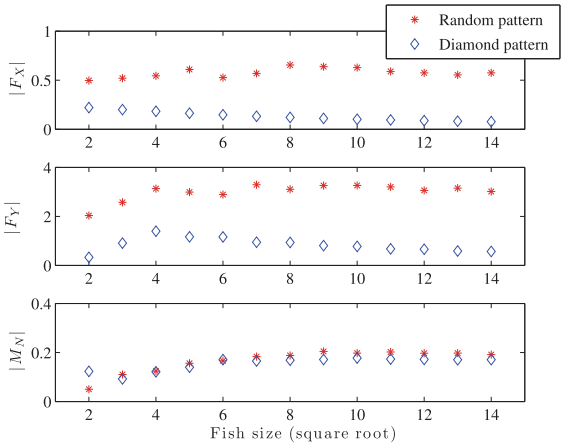

Fig. 3: (Colour online) Nondimensional hydrodynamic forces and moments as a function of the square root of the fish school size n (the fish school size is $n \times n$); for random ($*$) and diamond ($\diamond$) patterns. Top: longitudinal forces. Middle: lateral forces. Bottom: yawing moments.

sitions of the two bodies change in time as a quasi-steady approximation, where each position is calculated individually. The two bodies are separated by a lateral distance, η_{ij}, and fore-and-aft distance, ξ_{ij}, which is a function of time t. For each two bodies we define two coordinate systems, (x_i, y_i, z_i) fixed on body i and (x_j, y_j, z_j) fixed on the upper upstream neighbour, body j, which are related to the fixed coordinate system (x_0, y_0, z_0) so that

$$\begin{aligned} x_0 = x_i \ \ + U_i t = x_j + U_j t - \xi_{ij}(0); \\ y_0 = y_i \ = y_j + \eta_{ij}; \quad z_0 = z_i = z_j, \end{aligned} \tag{1}$$

and

$$\xi_{ij}(t) = x_j - x_i = (U_i - U_j)t + \xi(0), \tag{2}$$

where $\xi_{ij}(0)$ is the initial longitudinal distance between bodies i and j. The flow about the i-th body is considered asymptotically steady, and can be estimated by standard methods of slender body theory [15]. It is also assumed that the separation distance η_{ij} is $O(\epsilon L_i)$ to allow calculations of small lateral separation distances. Thus, the three-dimensional velocity potential in the outer region is expanded in a *Taylor* series about the other body. Using the method of asymptotic expansions we find a solution to the longitudinal motion. The inner solution is governed by the two-dimensional *Laplace* equation and the no-penetration boundary condition. The outer solution is governed by the three-dimensional *Laplace* equation and by the condition at infinity where the potential diminishes. These solutions are matched in an overlap region, leading to, after rather long but straightforward algebra, expressions for the longitudinal and lateral forces, and moment acting on body j due to the presence and/or movement of

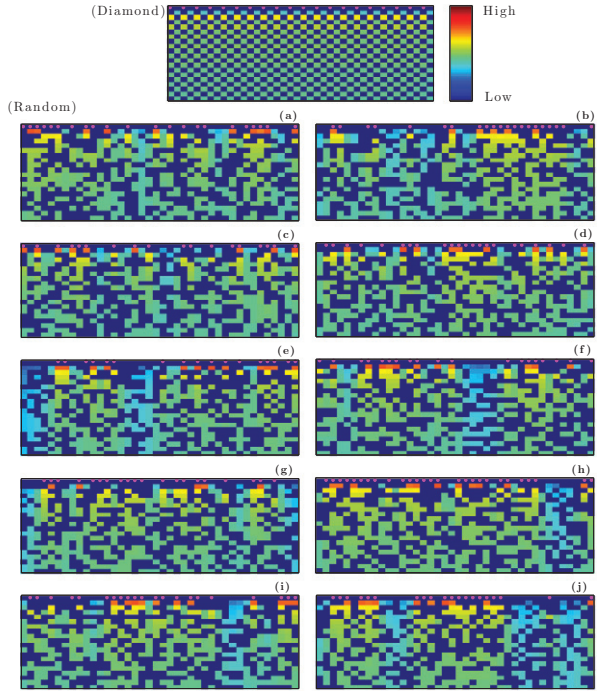

Fig. 4: (Colour online) The hydrodynamic force effect of the upper fish row (presented by •) on the remaining fish school. Force exerted on each individual fish: blue (low) to red (high). Upper subplot: diamond pattern. Remaining subplots: random patterns.

body i [1,2,15]:

$$X_j = \sum_{i=1}^{n} \frac{\rho}{4\pi} \int_{L_i} S_i'(x_i) \left[U_i^2 + U_j^2 \int_{L_j} S_i'(x_i) T_j(x_j) \sigma_{ij} \mathrm{d}x_j \right] \times \mathrm{d}x_j \mathrm{d}x_i, \tag{3}$$

$$Y_j = \sum_{i=1}^{n} \frac{\rho U_j \eta_{ij}}{4\pi} \int_{L_i} (2U_j - U_i) S_i'(x_i) \int_{L_j} T_j(x_j) \mathrm{d}x_j \mathrm{d}x_i, \tag{4}$$

$$N_j = \sum_{i=1}^{n} \frac{\rho U_j \eta_{ij}}{4\pi} \int_{L_i} [x_i(2U_j - U_i) S_i'(x_i) + 2U_j S_i(x_i)] \times \int_{L_j} T_j(x_j) \mathrm{d}x_j \mathrm{d}x_i \mathrm{d}x_i. \tag{5}$$

where n is the school size, $j = 1, 2, \ldots, n$, and $T_j(x_j) = S_j'(x_j)(\sigma_{ij}^2 + \eta_{ij}^2)^{-3/2}$; $\sigma_{ij} = (x_j - x_i - \xi_{ij})$; $S_j(x_j) = S_j(0)(1 - 4x_j^2/L_j^2)$, where $S_j(x_j)$ is chosen to be a simple sectional area distribution of parabolic form; $S_j(0)$ is a constant related to the cross-sectional area of the j-th body, $S_j' \equiv \mathrm{d}S_j(x)/\mathrm{d}x$ and $S_j(x_j) = \pi r_j^2$; and r_j is the radius of the cross-sectional area. For nondimensional representation we define $F_{X_j} \equiv X_j L^2/\rho U^2 S^2$; $F_{Y_j} \equiv Y_j L^2/\rho U^2 S^2$; $M_{N_j} \equiv N_j L/\rho U^2 S^2$.

Data collection and analysis. A total of 48 photos and eight videos (total duration: 300 seconds) of fish schools in the open sea (Red Sea) from 11 different species were ex-

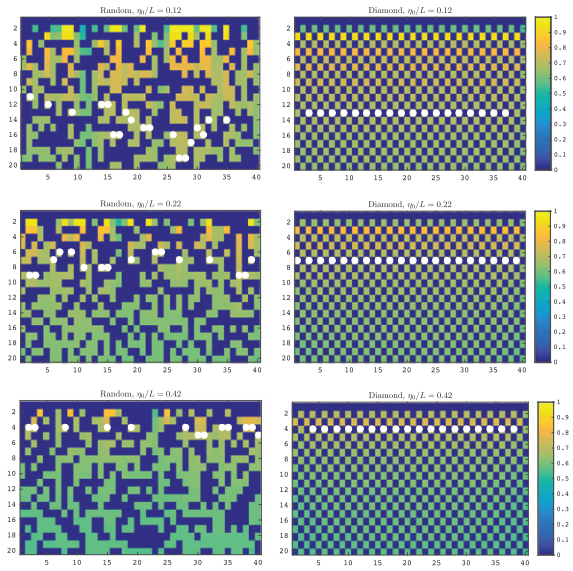

Fig. 5: (Colour online) The hydrodynamic force effect of the upper fish layer (not presented here) on the remaining fish school, for random and diamond cases with average lateral distances $\eta_0/L = 0.12$, 0.22, and 0.42 from top to bottom, respectively. Fish that experience *at least* a threshold force are represented by a white bullet.

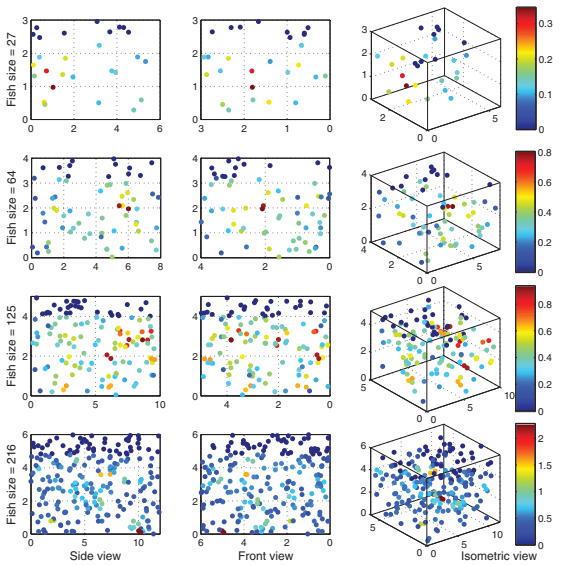

Fig. 6: (Colour online) The hydrodynamic force effect of the upper fish layer (presented by dark blue •) on the remaining fish school. Force exerted on each individual fish: blue (low) to red (high). Left: side views (fish move to the right). Middle: front views (fish move into the page). Right: isometric view. First row: 27 fish, in a $6 \times 3 \times 3$ box. Second row: 64 fish, in a $8 \times 4 \times 4$ box. Third row: 125 fish, in a $10 \times 5 \times 5$ box. Fourth row: 216 fish, in a $12 \times 6 \times 6$ box.

amined for analysis. Data presented in fig. 2 was processed from a movie (MPEG-4 format) which recorded movement and distribution of fish in a school for 00.59.36 min. The video was converted to TIF file formats (at 15 frames per second giving a total of 894 frames) using the tool iMovie (Mac). Positions (x and y coordinates) of fish were determined at three different frames (71, 86 and 104), corresponding to movement at times 00.04.00, 00.05.44 and 00.06.59 min, respectively, using image analysis software (SigmaScan Pro 5.0). The eyes of the fish were taken as reference points.

Table 1: Calculations of the mean total forces per school size for diamond and random patterns. In the case of a random pattern, the mean total forces are a factor of two to five times larger.

School size	Diamond	Random
2×2	0.3974	2.0754
3×3	0.9302	2.6132
4×4	1.4072	3.1733
5×5	1.1768	3.0591
6×6	1.1690	2.9400
7×7	0.9532	3.3220
8×8	0.9422	3.1863
9×9	0.8139	3.3187
10×10	0.7812	3.3280
11×11	0.6810	3.2530
12×12	0.6641	3.1084
13×13	0.5921	3.1943
14×14	0.5734	3.0777

In the case of figs. 3 and 4, the velocities and lengths of the fish were considered unity, and the slenderness parameter $\epsilon = 0.1$. For the diamond pattern cases the longitudinal and lateral distances between each two neighbouring fish rows and columns are $\xi_0/L = 1.1$, and $\eta_0/L = 0.12$, respectively. In the case of a random pattern mode, the same amount of fish was randomly distributed within a similar domain size; the longitudinal and lateral distances were calculated based on a *Monte Carlo* algorithm as presented in the statistical guidelines. In fig. 5, we considered $\eta_0/L = 0.12$, 0.22, 0.42 and a constant threshold force $F_{Y,\mathrm{th}}/F_{Y,\max} = 0.69$, where $F_{Y,\max}$ is the absolute maximum force in the figure. In the case of fig. 6, the algorithm was extended to three dimensions.

The random pattern data presented in fig. 3 were obtained by carrying out a *Monte Carlo* algorithm. Each data point represents an average of repeated random computations of a size of at least a hundred repetitions. For each school size, $n \times n$, the length and width of the computation domain, $\mathbf{l} \times \mathbf{w}$, are given by $\mathbf{l} = n \times L_i$, and $\mathbf{w} = n \times d$. The location of the fish are generated randomly, such that no overlaps are allowed. The longitudinal and lateral forces, and yawing moments between each two fish are computed using eqs. (3), (4), and (5). Note that the random pattern data presented in subplots (a)–(j) of fig. 4 are for a single calculation (no repetition). The (layer) school size is 20×20.

Results. – The analysis presented here considers two structural patterns: diamond and random. The mean longitudinal and lateral forces acting on a fish in a random pattern mode are larger than those in a diamond mode, whereas the mean moments are similar in both modes (fig. 3). In this respect, a diamond-shaped swimming pattern is optimal in terms of energy saving which supports previous findings by [8]. Such mode might be observed in schools migrating in "safe" zones, or in large fish or mammals, *e.g.*, dolphins [1,10], that use the saved energy for extra thrust during escape. However, smaller fish count on their manoeuvrability for survival, which increases with the total hydrodynamic forces [16,17]. Table 1 compares between the mean total hydrodynamic forces, $F_{tot} = \sqrt{F_X^2 + F_Y^2}$, of the two patterns. It indicates that the mean total force in random patterns is two to five times larger than in diamond patterns. Given that there is a hydrodynamic force threshold at which a fish can sense the instantaneous movement of another remote fish, swimming in a random pattern mode allows fish to interact at larger distances, resulting in a more efficient distribution of "information" transfer, from a hydrodynamic perspective. This can be seen by the following example. Assume a (layered) rectangular fish school of the size of 20×20 (fig. 4), the fish on the sides of the rectangle represent an envelope that separates the remaining fish from the surrounding. If, for the sake of brevity, the whole upper fish row (presented by •) encounters a danger, then the survivability of the whole school depends on how far the information is transferred at each instance through the whole school, again from a hydrodynamic perspective. In other words, we are interested in the distribution of the total hydrodynamic effect of the first fish row on the remaining fish school. In a diamond pattern mode (upper subplot) the effect on each row is almost homogeneous. While the lateral forces experienced by the second row are relatively small, due to the fact that ξ_{ij} is large, the effect is largest on the third row and the general trend is that the hydrodynamic forces decrease with the (double) rows. However, for random pattern modes (subplots (a)–(j)) higher forces penetrate through the rows, which can be seen in the figure by the differences in colour gradients across the vertical layers (*i.e.*, orange yellow and green compared to blue). As an example, if the sensitivity threshold force $F_{Y,\mathrm{th}}$ is presented by the forces on the fifth row of the upper subplot of fig. 4 —meaning that a change in the first row cannot be felt on rows 6 and further— larger forces can be found on rows 8–11 in the random cases. A quantitative comparison of the location of the most remote fish that experience the threshold force $F_{Y,\mathrm{th}}$ is given in fig. 5. In all presented cases we considered a constant $F_{Y,\mathrm{th}}$ with a value of 69% of the absolute maximum force, *i.e.*, $F_{Y,\mathrm{th}}/F_{Y,\max} = 0.69$ on the scale bars. For a relatively large average lateral separation distance $\eta_0/L = 0.42$, only few fish would experience the threshold force deeper in the fish school (reaching the fifth row), in the case of random structural pattern, compared to the diamond pattern where $F_{Y,\mathrm{th}}$ does not exceed the fourth row. Nevertheless, in the random case, some of the fish found on the fourth row experience larger forces compared to the diamond case. Obviously, taking the limit were $\eta_0/L \gg 1$ none of the fish will experience any threshold force, nor in random neither in diamond structural patterns. On the other hand, for smaller separation distances the effect becomes much more noticeable, whereby the threshold force penetrates through 6 more rows (*i.e.*, 30% of the whole school lateral size) in the case of random structural pattern with $\eta_0/L = 0.12$. Thus, the reaction at the next time instant would occur at multilevel rows simultaneously deeper in the school, which may enhance the overall manoeuvrability of the fish school as a whole.

Discussion. – Consider n fish of the first row exerting lateral forces on a fish at the furthest row k where the threshold force can still be experienced. Since $F_Y \propto \epsilon^2 L^2/\eta_0^2$, we can derive a relation of the threshold force as

$$F_{Y,\mathrm{th}} = \beta\epsilon^2 \frac{n^2 L^2}{k^2 \eta_0^2}, \tag{6}$$

where $\beta = 0.3228$ is the proportionality constant calculated from the numerical results, say for $\eta_0/L = 0.12$. Alternatively, we can write for the k-th row

$$k = \left\lfloor \sqrt{\frac{\beta}{F_{Y,\mathrm{th}}}} \frac{nd}{\eta_0} \right\rfloor \tag{7}$$

where the special brackets present the floor function. Relation (7) shows that the furthest row in which a fish may still feel the sudden movement of the fish in the first row decreases inversely with the square root of the force threshold, *e.g.*, if the fish sensitivity increases by two, the information would penetrate four times further away. Moreover, we see that fish that school at smaller average lateral separation distances, or have a less slender shape would contribute to further penetration of the information. Substituting the values of the other two cases $\eta_0/L = 0.22$, and 0.42 (given in fig. 5) into relation (7) we obtain $k = 10$, and 5, that are in agreement with the numerical results.

Note that as $\eta_0/L \ll 1$ the above relation is no longer valid and the exact lateral separation distance, $\eta = \eta(x_i, x_j)$ has to be considered, and thus a higher-order solution is required (see [2]). In this case, the lateral forces become even larger, and thus one expects the threshold force to penetrate deeper in the school. This analysis is important when the characteristic school size is much greater than the penetration distance. However, even if the characteristic school size is relatively small, within a random structural pattern a manoeuvring fish experiences, on average, larger centripetal forces, and thus can reach larger angular velocities ($\omega \propto {F_{tot}}^{1/2}$). Since each fish, within a random pattern, applies on average larger hydrodynamic forces on the school, its manoeuvring, *e.g.*, as a response

to danger, results in larger impact on the fish school and in particular on its proximate neighbours. Therefore, the hydrodynamic changes within the school as a whole are larger in case of random pattern mode, which may enhance its survivability. Note that the mathematical analysis presented in fig. 4 considers discrete layers of the school, an assumption which is rarely met in Nature [4,18,19]. However, it is easy to show that the three-dimensional fish school analysis would result in larger hydrodynamic forces, and thus a change in movement can be felt more remotely and it is likely to further enhance the school manoeuvrability, and alertness. Such an analysis is carried out in fig. 6. Here, we examined the three-dimensional effect of the upper fish group (presented in dark blue •) on the remaining school members. We considered four different school sizes, 27, 64, 125, and 216, within boxes of dimensions $6\times3\times3$, $8\times4\times4$, $10\times5\times5$, and $12\times6\times6$, respectively. The fish swim from left to right relative to the side view. The hydrodynamic effects made by the upper fish group on the remaining school members are somewhat disordered, which can be seen by the inhomogeneous distribution of colours. It is also notable that the analysis of the videos show that the different fishes, of each school, may have different lengths, speeds, and orientations, (*e.g.*, [20]) as well as locomotion techniques that create wakes and vortices in a much more complicated flowfield, which may all add to the disordered behaviour of transferring the hydrodynamic "information" among the school members spatially.

The analysis made here has been described in the context of specific fish schooling species, though similar analysis can be carried out for other fishes, swarming behaviour in general, and bird flocking in particular, *e.g.*, by a straightforward extension of the work by [21], and [22]. The work presented here can also be applied for interaction between multiple AUVs with a submarine, *e.g.*, [23]. Finally, our findings support the general hypothesis that a disordered and nontrivial collective behaviour of individuals within a nonlinear dynamical system is essential for optimising transfer of information —an optimisation that might be crucial for survival.

* * *

The authors gratefully acknowledge Martina and Herbert Bauder for providing the photos and videos.

REFERENCES

[1] Kadri U., *The Flow Field and Forces on Two Slender Bodies Moving in Close Proximity*, M.Sc. Thesis, Technion Libraries, Israel Institute of Technology, Haifa (2005).
[2] Kadri U. and Weihs D., *J. Mar. Sci. Technol.*, **20** (2015) 249.
[3] Rattanasiri P., Wilson P. A. and Phillips A. B., *Ocean Eng.*, **80** (2014) 25.
[4] Partridge B. L. and Pitcher T. J., *Nature*, **279** (1979) 418.
[5] Partridge B. L. and Pitcher T. J., *J. Comp. Physiol.*, **135** (1980) 315.
[6] Killen S. S., Brown J. A. and Gamperl A. K., *J. Anim. Ecol.*, **76** (2007) 814.
[7] Killen S. S., Marras S., Steffensen J. F. and McKenzie D. J., *Proc. R. Soc. B*, **279** (2011) 814.
[8] Weihs D. and Webb P. W. (Editors), *Optimization of Locomotion in Fish Biomechanics* (Praeger, New York) 1983, pp. 339–371.
[9] Hemelrijk C. K. and Hildenbrandt H., *Interface Focus*, **2** (2012) 726.
[10] Weihs D., *J. Biol.*, **3** (2004) 8.
[11] Hamilton W. D., *J. Theor. Biol.*, **31** (1971) 295311.
[12] Tuck E. O. and Newman J. N., *Hydrodynamic interactions between ships*, in *Proceedings of the 10th Symposium on Naval Hydrodynamics*, edited by Cooper R. D. (Academy, Washington DC) 1974, pp. 35–70.
[13] Wang S., *J. Waterways Harbors Coast. Eng. Div.*, **101** (1975) 247.
[14] Wu T. Y. and Chwang A. T., *Double-body flow theory – A new look at the classical problem*, in *Proceedings the 10th Symposium on Naval Hydrodynamics*, edited by Cooper R. D. (Academy, Washington DC) 1974, pp. 89–106.
[15] Newman J. N., *Marine Hydrodynamics*, 3rd edition (The MIT Press, Cambridge, Mass.; London, England) 1977.
[16] Wu J. C., *AIAA J.*, **19** (1981) 432.
[17] Liu G., Yu Y.-L. and Tong B.-G., *Phys. Rev. E*, **84** (2011) 056312.
[18] Breder C. M., *Zoologica*, **50** (1965) 97.
[19] Oshima Y., *Bull. Jpn. Soc. Sci. Fish.*, **16** (1950) 195.
[20] Pitcher T. J. and Parrish J. K., *Behaviour of Teleost Fishes* (Springer) 1993, ISBN 978-0-412-42930-9, p. 415.
[21] Higdon J. J. L. and Corrsin S., *Am. Nat.*, **112** (1978) 727.
[22] Higdon J. J. L., *Induced Drag in Formation Flight*, S.M. Thesis (Johns Hopkins University) 1975.
[23] Leong Z. Q., Ranmuthigala D., Penesis I. and Nguyen H., *Ocean Eng.*, **106** (2015) 175.